UNDERSTANDING AND MODELLING WAVE-DRIVEN MIXED SAND TRANSPORT

J.J. van der Werf[1,2], F. Staudt[3], D. Posanski[3], W. van de Wardt[2], J. van der Zanden[2], B. Vermeulen[2], J.S. Ribberink[2] and S. Schimmels[3]

1. *Marine and Coastal Systems, Deltares, P.O. Box 177, 2600 MH, Delft, The Netherlands. jebbe.vanderwerf@deltares.nl*
2. *Marine and Fluvial Systems group, University of Twente, Drienerlolaan 5, 7522 NB Enschede, The Netherlands. willekevdwardt@gmail.com, j.v.d.zanden@marin.nl, b.vermeulen@utwente.nl, j.s.ribberink@utwente.nl*
3. *Forschungszentrum Küste, Leibniz University Hannover & Technical University Braunschweig, Merkurstraße 11, 30419 Hannover, Germany. staudt@fzk.uni-hannover.de, posanski@fzk.uni-hannover.de, schimmels@fzk.uni-hannover.de*

Abstract: This paper presents new net transport data from the STENCIL full-scale wave flume experiments with a sediment mix of a fine (0.21 mm) and a coarse (0.58 mm) sand fraction. These and existing mixed sand transport data from full-scale oscillatory flow tunnel experiments were used to validate the SANTOSS practical sand transport formula, which includes size-selective transport mechanisms and hiding and exposure effects. The STENCIL data show a strong effect of the sediment mix on the bed form regime and net transport rates. The SANTOSS formula predicts the flow tunnel net sand transport data well, and does a reasonable job in reproducing the net sand transport per fraction in the mix. The new STENCIL net transport data are generally underpredicted. In further research the SANTOSS formula will be further tested and improved using more detailed STENCIL data of flow and sand transport processes.

Introduction

The majority of the world's coastal regions comprise heterogeneous (mixed) rather than homogenous (uniform) sedimentary environments. Transport rates of mixed sediments may be substantially different from transport rates of uniform sediments. This may affect coastal evolution such as beach accretion during mild wave conditions and erosion during storm events.

A first difference between mixed and uniform sands originates from the non-linear dependence of sediment transport on particle diameter, which is mainly true for suspended load. This implies that a multi-fraction modelling approach generally leads to a higher sediment transport than a single-fraction approach. This effect increases with the width of the size distribution (see Van Rijn, 2007).

Another important mixed sediment effect is hiding and exposure (HE). Coarser particles within a mix are more exposed to the flow, whereas smaller particles can "hide" between the larger particles. This results in an increased mobility of

coarser and a reduced mobility of finer grains within a mix. On the basis of large-scale oscillatory flow tunnel experiments, Hassan & Ribberink (2005) showed that coarse/fine sand fractions contribute up to 3 times more/less to the total net transport than would be expected from the sediment bed availability.

Furthermore, size-selective transport leads to horizontal (mainly cross-shore) and vertical bed sorting. There is typically a coarsening towards the shoreline related to offshore suspended transport of mainly fines due to undertow, and a relatively large coarse grain contribution to the onshore-directed bedload due to wave skewness (Broekema et al., 2016; Van der Zanden et al., 2017).

Kinematic sorting of sizes, where small grains tend to move downward and fill the pore space between large grains, which move upward, can result in an upwards fining (Kleinhans, 2004; Hassan & Ribberink, 2005). In unidirectional flows (like in rivers) finer particles are generally dominating in the upper layers and coarser particles are dominating in the lower layers. This means that coarse particles are generally present in troughs of river dunes (see e.g. Blom et al., 2003).

Engineering morphological models (e.g. Delft3D, XBeach) are frequently used in coastal engineering practice. These include relatively simple and practical empirical formulas to compute net sand transport and usually assume that the seabed consists of one single-size sediment. In a multi-fraction approach, some of the relevant sediment mixing effects are accounted for in a parameterized way. However, these are based on limited experimental data, none of which has come from controlled laboratory experiments involving sediment mixtures under large-scale waves.

As a result, it is questionable to use these models to support design and management decisions for the coastal zone with heterogeneous sediments. This applies in particular to the planning and monitoring of coastal nourishments, as the properties of the nourishment (size and grading) can deviate substantially from the native sand. Understanding and modelling of cross-shore sediment sorting is also important to assess the suitability of the seabed for benthic species that have a grain-size preference.

The lack of reliable full-scale data hampers the understanding and modelling of wave-driven mixed sediment dynamics. This paper presents new net mixed sand transport data from full-scale wave flume experiments. The new and existing data are used to assess the SANTOSS practical sand transport formula (Van der A et al., 2013).

STENCIL experiments

Experimental set-up

Sediment transport experiments with different sand mixtures were conducted in the Large Wave Flume (Großer Wellenkanal/GWK; 300 m length, 5 m width, 7 m depth) at Forschungszentrum Küste (FZK) in Hannover, Germany. A horizontal test section of approximately 0.9 m in height (0.6 m foundation plus 0.3 m sand bed) and 30 m in length was set up at a distance of roughly 97 m from the wave paddle. The test section was sloped at both the onshore and offshore end to create a gradual transition of the water depth. The water depth in the flume was 4.4 m in all experimental runs, i.e. approximately 3.5 m above the initial sand bed. One wave gauge, three pressure transducers and a vertical array of three Acoustic Doppler Velocimeters (ADVs) were used to monitor the wave parameters along the test section. Further instrumentation was used, but this is not subject of this paper.

Table 1 shows the experimental conditions. The tested sediment consisted of well sorted fine ($D_{50,\mathrm{fine}}$ = 0.21 mm) and coarse sand ($D_{50,\mathrm{coarse}}$ = 0.58 mm) in four different mixing ratios, with different median ($D_{50,\mathrm{mix}}$) and mean (D_{m}) grain-sizes of the mix. Each test bed was subjected to two regular wave conditions. The velocity skewness ranged from $R = U_{\mathrm{on}}/(U_{\mathrm{on}} + U_{\mathrm{off}})$ = 0.61 to 0.64, with U_{on} and U_{off} the onshore and offshore orbital velocity peaks, respectively. The acceleration skewness was minor. For each experiment, waves were generated in five series ("runs") of 200 waves (= 1400 s). Despite identical wave paddle stroke and water depth, the flow velocities at the test section varied slightly in between experiments of the same wave condition. The bed morphology changed significantly depending on the sand mixture, which resulted in variations in wave height and shape at the test section.

Table 1. Conditions STENCIL experiments.

Test	**Sand**	**P_{fines} (%)**	**$D_{50,\mathrm{mix}}$ (mm)**	**D_{m} (mm)**	**Wave condition**	***H* (m)**	***T* (s)**
0516	A	100	0.22	0.21	WC1	1.5	7.0
0518					WC2	1.0	7.0
0525	B	68	0.24	0.33	WC1	1.5	7.0
0530					WC2	1.0	7.0
0605	C	46	0.44	0.41	WC1	1.5	7.0
0608					WC2	1.0	7.0
0615	D	26	0.57	0.48	WC1	1.5	7.0
0620					WC2	1.0	7.0

Before the start of the experiment as well as after every wave run, bed profiles were recorded at four transects (y = 3.0 m, 3.5 m, 4.0 m and 4.5 m) using single-beam echo sounders (Figure 1). To avoid interference between the echo sounders and the instrument frame no profiles were recorded at y = 0–2.5 m. The distance between the echo sounders and the undisturbed sediment bed was 0.5 m. The echo sounders were attached to a mobile platform and moved over the sediment bed at a constant velocity and recorded a profile with a horizontal resolution of 2.4 cm. The instruments have a vertical resolution of 1 mm.

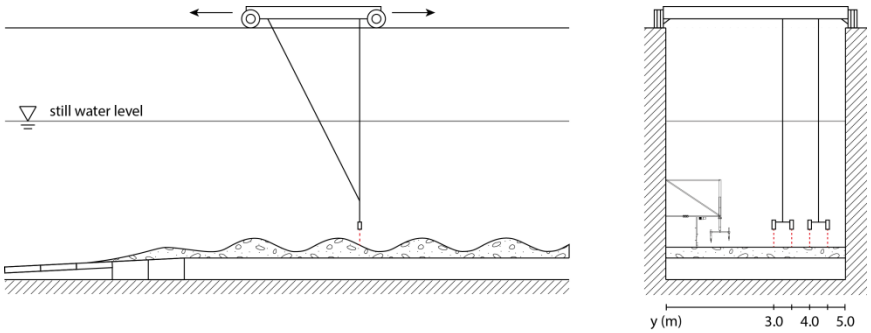

Figure 1. Sketch of the echo sounder setup used to record the bed morphology before and after each wave run. Left: side view; right: view towards the wave paddle.

Data-analysis

As the bed compacted significantly in the beginning of the experiments the initial profile before the first run (#00) was excluded from the subsequent data analysis. For the remaining profiles #01-#05 the hydrodynamic data (wave gauge, pressure transducers, and ADVs) were phase-averaged, neglecting the irregular first and last waves.

The bed profiles were referenced using horizontal marker bars at fixed x-positions in the flume, with x defined positively shoreward from the wave paddle in rest position. The profiles were analyzed in the range of $x \approx 88$–140 m, i.e. from approximately 8 m offshore of the test section to approximately 13 m beyond the onshore end of the test section. After cleaning the profile data from erroneous spikes the net transport rate was calculated by applying the Exner equation, which is based on the mass conservation principle, to each data point of the profile:

$$q_s(out) - q_s(in) = (1 - \varepsilon_0)\frac{dV}{dt} \quad (1)$$

with sediment transport rate q_s (m^2/s), bed porosity ε_0 (-), volume change dV (m^2) and elapsed time dt (s). For simplicity, the porosity was set to a constant value of 0.4. Assuming no volume change in the longshore direction (i.e. a two-dimensional bed morphology), $dV = \Delta x * \Delta z$ with a horizontal profile resolution Δx = 2.4 cm and an elevation change of $\Delta z = (z_{start} - z_{end})$. dt = 5600 s denotes the time elapsed between profile recordings #01 (after the 1st wave run) and #05 (after the 5th wave run).

This equation can be solved starting at either the offshore (left) or onshore (right) end of the profile with q_s = 0 m^2/s as boundary condition. Provided that all the transported material is recorded in the bed profiles and that no three-dimensional bed forms, variations in bed compaction or measurement inaccuracies exist, the left- and right-hand side estimates are identical. In practice, the aforementioned assumptions are not fully valid, resulting in deviations between the left- and right-hand estimates. As the accuracy of each estimate is considered to decrease with distance from its respective starting point, a weighted average of both estimates is used. This weighted average requires two boundary conditions ($q_{s,on} = q_{s,off}$ = 0 m^2/s), which implies that any given "volume loss" is not caused by material transported out of the test section, but by bed compaction and the earlier described reasons.

The weighted result is considered as the lower limit estimate of the net sand transport, because sediment deposits beyond the onshore end of the profiling range (x > 140 m) were occasionally observed. This implies that the zero onshore transport boundary (as assumed in the weighted average approach) is not correct in all cases, which results in an underestimation of the total net sand transport. The result of the integration starting at the offshore end is considered as the upper limit of the net sand transport estimate. The actual net transport rate lies in between these two limits and is therefore shown as the average of both estimates.

The net sand transport was calculated for each echo sounder transect separately and then averaged over all four transects to yield a final mean value. Furthermore, the net transport rates were averaged over 4 m distance around the center of the test section.

The ripple dimensions (length λ and height η) were extracted from the echo sounder profiles (in the range of x = 98–125 m) and averaged over the four transects.

Experimental results

Bed morphology

The sediment bed remained plane in the first experiments with unimodal, fine-grained sand (Tests 0516 and 0518) indicating sheet-flow regime (Figure 2). Bed forms started to develop with the addition of coarse sand. Under the higher waves of WC1, Sand B (68% fines, Test 0525) remained generally plane in the central 10 m of the test section, but showed large bed forms on the side slopes of the test section. The lower WC2 (Test 0530) led to the development of large morphological irregularities throughout the test section. However, due to the high irregularity bedform dimensions were not quantified. The absence of detectable ripples indicates that Sands A and B were mostly transported in the sheet-flow and transitional regime (sheet-flow on top of large bed forms).

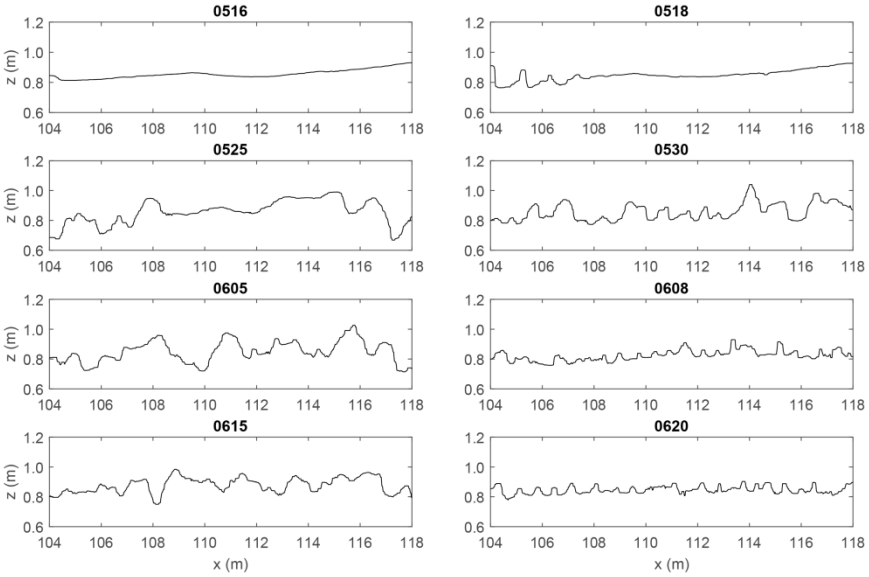

Figure 2. Final bed profiles (#05) at transect y = 3.0 m for all experiments.

Sand C (46% fines) developed large ripples (λ > 100 cm; $\eta \approx 11$ cm) under the high WC1 (Test 0605). The same sand mixture developed smaller, more regular ripples (λ = 70 cm; η = 6 cm) under WC2 (Test 0608). Ripple dimensions of Sand D (26% fines) were similar to those in Test 0608: WC1 led to slightly

larger ripples (λ = 83 cm; η = 7 cm), while WC2 generated ripples with λ = 72 cm and η = 6 cm. The development of bed forms in the last four experiments (Sands C and D) indicates that sediment transport occurred mainly in the ripple regime. In general, bedform showed a higher variability in the experiments with higher waves, whereas they were more regular in the lower wave regime.

Net sand transport rates

Figure 3 shows the measured total net sand transport rates. As expected, the higher waves (H = 1.5 m) resulted in higher net transport rates than the lower waves (H = 1.0 m). For both wave conditions, the net transport rate generally increases with the amount of fine sediment in the bed. The maximum net transport rate, however, was recorded in experiment 0525 with Sand B (68% fines) instead of 0516 with Sand A (100% fines).

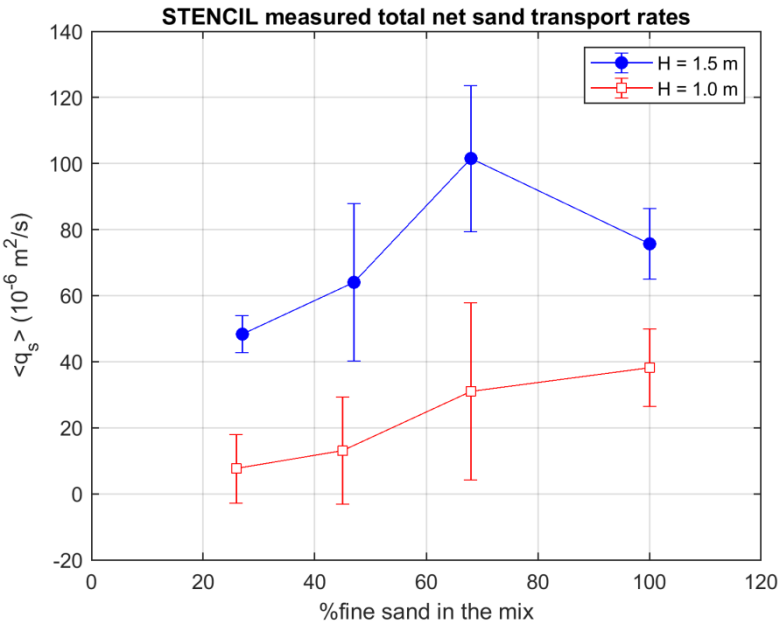

Figure 3. Total net sand transport rates from the STENCIL experiments.

The total net sand transport rates for Sand A (100% fines) are higher than measured by Schretlen (2012) (cases Re1575m, Re1565m; Re1065m) and Dohmen-Janssen et al. (2002) (cases Mi and Mh) in the same wave flume with

comparable wave and sand conditions. This applies especially to the 1.0 m wave condition.

Validation SANTOSS practical sand transport formula

SANTOSS formula

The SANTOSS formula is a practical sand transport formula for non-breaking waves and currents (Van der A et al., 2013). It computes the total net sand transport within the wave bottom boundary layer. It does not account for transport at higher elevations above the bed. It is based on the semi-unsteady, half wave-cycle concept, with bed shear stress as the main forcing parameter. It accounts for unsteady phase-lag effects between velocities and concentrations and progressive surface wave effects. The formula is developed using a database of 226 net transport rate measurements from large-scale oscillatory flow tunnels and a large wave flume, covering a wide range of full-scale flow conditions and uniform and graded sands.

For graded sands the ripple dimensions and sheet-flow layer thickness are computed for the mixture as a whole. The grain-related roughness, (critical) bed shear stress, phase lag parameters and transport contributions are computed per sediment fraction. Following Van Rijn (2007), HE effects are accounted for through a correction of the bed shear stress with the following factor:

$$\varepsilon_{eff,j} = \left(\frac{d_j}{d_{mix}} \right)^{0.25} \tag{2}$$

with d_j the grain-size per fraction and d_{mix} the representative grain-size of the sand mix.

Comparison with data from oscillatory flow tunnel experiments

First, the SANTOSS formula will be compared with data of net transport of mixed sands from large oscillatory flow tunnel experiments (Hamm et al., 1998; Hassan, 2003; O'Donoghue & Wright, 2004). These are 19 bi- and tri-modal sediment cases with a mean grain size between 0.22 and 0.44 mm. The full-scale wave conditions include orbital motion (sinusoidal, velocity-skewed, acceleration-skewed) with and without a following net current. All cases were in the plane-bed, sheet-flow regime with limited suspended load. These data were

used to develop the SANTOSS model. Other than Van der A et al. (2013), we will also compare the formula to the net sand transport per fraction.

Table 2 shows the error statistics for the total net sand transport rates. This includes the Brier Skill Score (BSS), *bias*, squared coefficient of correlation (r^2) and the percentage of cases computed within a factor of 2 and 10 differences. It includes the uniform and graded SANTOSS approach with a median (default) and mean representative grain-size, and calculations where HE effects were switched off.

Table 2. SANTOSS formula performance criteria based on comparison against 19 cases of net mixed sand transport from oscillatory flow tunnel experiments.

Model setting	**BSS (-)**	**Bias (%)**	r^2 **(-)**	**Fac2 (%)**	**Fac10 (%)**
Uniform, $D_{50,mix}$	-0.28	-101	0.60	74	74
Graded, $D_{50,mix}$	0.90	-11	0.87	84	95
Graded, D_m	0.83	-15	0.71	79	89
Graded, no HE effects	0.76	-35	0.70	79	84

The best agreement is obtained with the default SANTOSS graded formula settings. Note that the error statistics differ somewhat from those presented in Van der A et al. (2003), because of later formula improvements. Agreement between formula and data is "excellent" in terms of BSS, according to the qualification of Van Rijn et al. (2003). The uniform approach has no skill (BSS < 0), and model performance decreases when using another representative grain-size and when ignoring hiding and exposure effects. Although occasionally the direction of net transport of the fine sand fraction is predicted incorrectly, the SANTOSS formula does a reasonable good job in computing the transport rates per fraction (Figure 4).

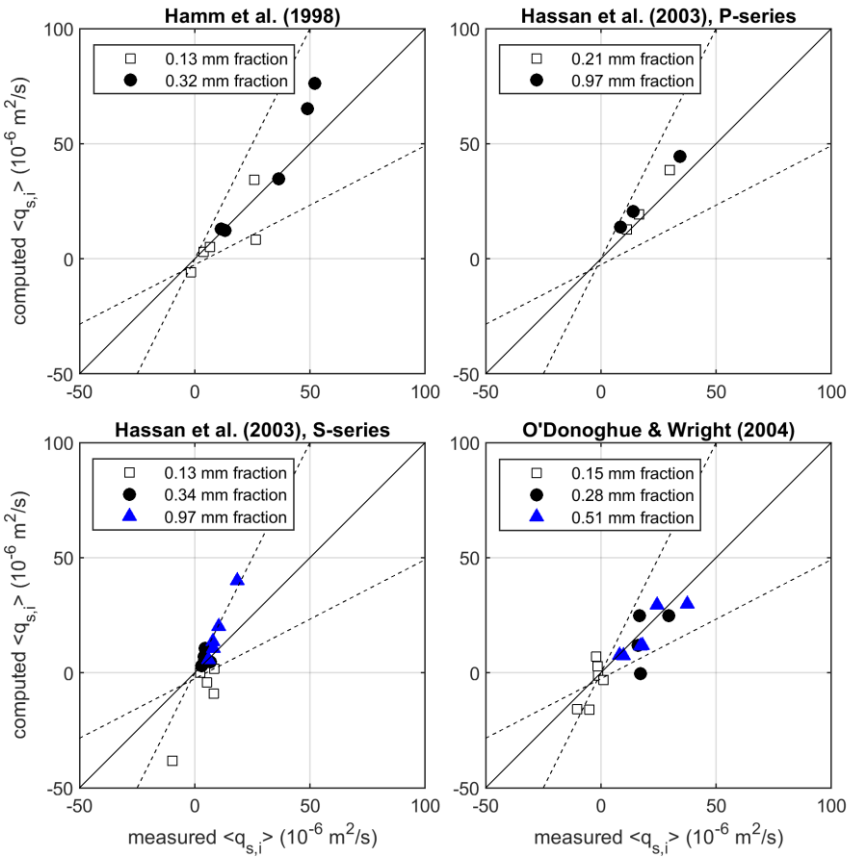

Figure 4. Measured and SANTOSS computed net sand transport per fraction in the mix. The solid lines denote perfect agreement and the dashed lines a factor of 2 difference.

Comparison with STENCIL data

Table 3 and Figure 5 compare measured and SANTOSS computed net transport rates for the STENCIL experiments. The graded approach gives better results than the uniform approach. HE effects and the choice of representative grain-size do not have a very large effect on the SANTOSS model results. Using the mean grain-size as representative for the mix improves model performance for the Sand D (26% fines), WC1 case, which is largely overpredicted using the median grain-size. The mean grain-size of Sand D is 0.48 mm, and the median

grain-size is 0.57 mm. As a result, the SANTOSS formula with the mean grain-size computes a thinner sheet-flow layer and smaller ripples, and hence a lower bed roughness and transport rate.

Table 3. SANTOSS formula performance criteria based on comparison against 8 cases of net mixed sand transport from the STENCIL experiments.

Model setting	**BSS (-)**	**Bias (%)**	**r^2 (-)**	**Fac2 (%)**	**Fac10 (%)**
Uniform, $D_{50,mix}$	0.48	-30	0.15	38	75
Graded, $D_{50,mix}$	0.64	-42	0.28	38	88
Graded, D_m	0.67	-52	0.46	50	75
Graded, no HE effects	0.61	-47	0.26	38	75

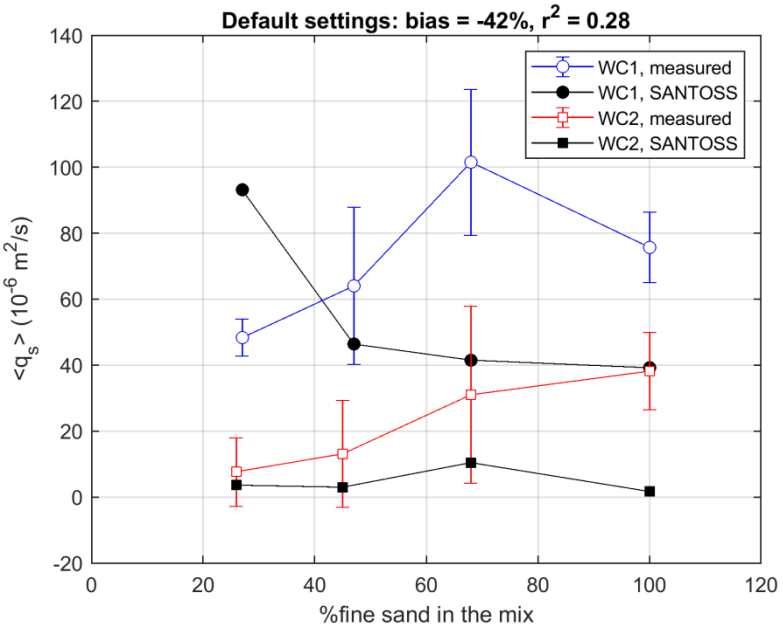

Figure 5. Comparison between measured and SANTOSS computed net sand transport for the STENCIL experiments.

Although the model performance indicators are not as good as for the comparison against the flow tunnel data (Table 2), the BSS is still "good" according to the Van Rijn's qualifications and 88% of the STENCIL cases is predicted within a factor of 10. The negative bias indicates a general underprediction.

The STENCIL data provide the total net sand transport, including both bedload and suspended load. The SANTOSS formula computed the total near-bed load, approximately the lowest 0.1 m near the bed. In the case of high sediment suspension (fine sands, rippled beds) in combination with wave-driven current (e.g. undertow), there can be a significant amount of current-related suspended load above the boundary layer, which is not captured by the SANTOSS formula. A first rough estimate, based on the wave-averaged concentration measurements and an estimated current profile, suggests that this current-related suspended load component is probably not very important for the plane-bed, sheet-flow cases (Sands A and B), but can be for the rippled-bed cases (Sands C and D).

Conclusion

1. The new STENCIL GWK data show the importance of the ratio of the coarse (0.58 mm) and fine (0.21 mm) sand fraction in the mix on the bed morphology. For offshore wave heights of 1.0 and 1.5 m, the plane-bed/sheet-flow regime prevailed for the mixes with 68% and 100% of fine sand, whereas ripples developed for the mixes with 26% and 46% of fine sand.

2. The higher waves (H = 1.5 m) resulted in higher net transport rates than the lower waves (H = 1.0 m), and the net transport rate generally increases with the amount of the fine sand in the bed.

3. The SANTOSS formula predicts the flow tunnel net sand transport data well, and does a reasonable job in reproducing the net sand transport per fraction in the mix. Agreement with the new STENCIL data is less convincing; there is a tendency of underprediction.

4. The SANTOSS graded approach agrees far better with the experimental data than a uniform approach. Including HE-effect improves model performance. There is only a small effect of using either the median or mean as representative grain size.

Other than the flow tunnel data, the STENCIL data included cases with rippled-beds and cases with potentially a significant suspended load transport

contributions above the wave boundary layer, which is not accounted for in the SANTOSS formula. In further research we will estimate the different transport contributions, allowing for a better understanding and a more fair comparison with the SANTOSS formula. We will also validate how (measured) ripple dimensions and sheet-flow layer thicknesses affect computed transport rates. A possible model improvement could be to compute the bed roughness for the sediment as a mix, instead of per fraction.

Acknowledgements

The work described in this publication was supported by the European Community's Horizon 2020 Programme through the grant to the budget of the Integrated Infrastructure Initiative HYDRALAB+, Contract no. 654110, and by the German Federal Ministry of Education and Research (BMBF) through the project STENCIL, contract no. 03F0761.

References

Blom, A., Ribberink, J.S., de Vriend, H.J. (2003). Vertical sorting in dunes, Flume experiments with a natural and a tri-modal sediment mixture. Water Resour. Res. 39 (2), 1025. doi: 10.1029/2001WR001088.

Broekema, Y.B., Giardino, A., Van der Werf, J.J., Van Rooijen, A.A., Vousdoukas, M.I., Van Prooijen, B.C. (2016). Observations and modelling of nearshore sediment sorting processes along a barred beach Profile. Coastal Engineering, 115, 50-62.

Dohmen-Janssen, C.M., Hanes, D.M. (2002). Sheet flow dynamics under monochromatic nonbreaking waves. Journal of Geophysical Research, 106 (C10), 3149, doi:10.1029/2001JC001045.

Hamm, L., Katapodi, I., Dohmen-Janssen, M., Ribberink, J.S., Samothrakis, P., Cloin, B., Savioli, J.C., Chatelus, Y., Bosboom, J., Nicholson, J., Hein, R. (1998). Grain size, gradation and density effects on sediment transport processes in oscillatory flow conditions. Data report, Part I. WL|Delft Hydraulics, the Netherlands.

Hassan,W.N.M. (2003). Transport of size-graded and uniform sediments under oscillatory sheet-flow conditions. PhD thesis, University of Twente, the Netherlands.

Hassan, W.N., Ribberink, J.S. (2005). Transport processes of uniform and

mixed sands in oscillatory sheet flow. Coastal Engineering 52, 745-770. doi:10.1016/j.coastaleng.2005.06.002

Kleinhans, M.G. (2004). Sorting in grain flows at the lee side of dunes. J. Earth Sci. 65, 75– 102.

O'Donoghue, T., Wright, S. (2004). Concentrations in oscillatory sheet flow for well sorted and graded sands. Coastal Engineering 50, 117–138.

Schretlen, J.L.M. (2012). Sand transport under full-scale progressive surface waves. PhD thesis, University of Twente, The Netherlands.

Van der A, D.A., Ribberink, J.S., Van der Werf, J.J., O'Donoghue, T., Buijsrogge, R.H., Kranenburg, W.M (2013). Practical sand transport formula for non-breaking waves and currents. Coastal Engineering, 76, 26–42.

Van der Zanden, J., Van der A, D.A., Hurther, D., Cáceres, I., O'Donoghue, T., Hulscher, S.J.M.H. Ribberink, J.S. (2017). Bedload and suspended load contributions to breaker bar morphodynamics. Coastal Engineering, 129, 74–92.

Van Rijn, L.C. (2007). Unified view of sediment transport by currents and waves, III: Graded beds. Journal of Hydraulic Engineering, 133(6): 761-775.

Van Rijn, L.C., Walstra, D.J.R., Grasmeijer, B., Sutherland, J., Pan, S., Sierra, J.P. (2003). The predictability of cross-shore bed evolution of sandy beaches at the time scale of storms and season using process-based Profile models. Coastal Engineering 47, 295–327.